SciMedCentral

Journal of Pharmacology & Clinical Toxicology

Research Article

In silico Modeling of New C-12 Substituted-14-Deoxy-Andrographolide Derivatives as Potent Anticancer Leads

Swayamsiddha Kar[1], Sai Manohar Chelli[1], Sai Giridhar Sarma Kandanur[1], Srinivas Nanduri[2], Siva Kumar Belliraj[1], and Nageswara Rao Golakoti[1]*

[1]*Department of Chemistry, Sri Sathya Sai Institute of Higher Learning, India*
[2]*Department of Process Chemistry, National Institute of Pharmaceutical Education and Research, India*

***Corresponding author**
Golakoti Nageswara Rao, Department of Chemistry, Sri Sathya Sai Institute of Higher Learning, Prasanthi Nilayam-515134, Andhra Pradesh, India, Tel: 91 9492595462; Email: gnageswararao@sssihl.edu.in

Submitted: 23 May 2017

Accepted: 12 June 2017

Published: 15 June 2017

ISSN: 2333-7079

Keywords
- Andrographolide
- Molecular modeling
- Docking
- Structure-activity relationship
- Active site study

Abstract

Many reports have shown that Andrographolide and its derivatives possess notable anti-cancer activity. In this study, we present the molecular docking studies of some newly synthesized C-12 substituted-14-deoxy-andrographolide derivatives. This helped to evaluate the probable targets of action responsible for the observed *in vitro* anti-cancer activity. This work delineates the role of the interacting amino acids residues in the active site. Consequently, the *structure activity relationship* (SAR) helps in drug design by demonstrating the effect of the C-12 substituent on the target site drug interaction. Finally, the compliance to Lipinski's parameters demonstrates their potential as promising leads in further anti-cancer drug development.

ABBREVIATIONS

EGFR: Epidermal Growth Factor Receptor; CDK: Cyclin-Dependent Kinase; MOE: Molecular Operating Environment; Ala: Alanine; Arg: Arginine; Asn: Asparagine; Asp: Aspartic acid; Cys: Cysteine; Gln: Glutamine; Glu: Glutamic acid; Gly: Glycine; Ile: Isoleucine; Leu: Leucine; Lys: Lysine; Met: Methionine; Phe: Phenylalanine; Pro: Proline; Ser: Serine; Thr: Threonine; Tyr: Tyrosine; Val: Valine

INTRODUCTION

Andrographolide, a labdane diterpenoid is the principal bioactive component of *Andrographis paniculata* (Acanthaceae) [1], has been reported to exhibit plethora of biological properties [2-6]. The promising anti-cancer activity shown by andrographolide has received wide attention over the years resulting in the synthesis and biological evaluation of a number of novel analogues. Studies have shown that andrographolide derivatives possess notable anti-cancer activity [7-24]. We focused our research efforts in evaluating the effect of introducing various substituents (alkyl amines, benzyl amines, phenyl thio and substituted aryl amines) at C-12 position of andrographolide on the anti-cancer activity. In this regard, we have synthesized a library of C-12-substituted-14-deoxy andrographolide derivatives (Figure 1) and submitted to National Cancer Institute (N.C.I.), U.S.A for the *in vitro* screening. Twelve of the analogues selected by NCI were evaluated against 60 human cancer cell line panel across 9 different cancer types at the National Cancer Institute (N.C.I.), USA. The results have already been reported by our group [25].

Since these analogues showed very good *in vitro* activity across the studied cell lines, we have explored their probable site of target binding via *in silico* simulations in this study. The minimal reports on the computational studies on andrographolide and its derivatives [26,27], also further encouraged us to pursue this study. In this regard, we have docked the synthesized derivatives with three different proteins namely Epidermal Growth Factor Receptor (EGFR) tyrosine kinase, Lung Cancer-Derived EGFR kinase and cyclin-dependent kinase (CDK)-5.

The EGFR kinases were chosen based on the literature reports [28], citing the over expression of EGFR in a significant number of human tumors e.g. breast, ovarian, colon, renal and prostate. Over-expression of EGFR family receptors has always been observed in these tumors (60% approximately) [28]. The cyclin-dependent kinases (CDK) CDK1, CDK2, CDK4, and CDK6 are serine/threonine protein kinases targeted in cancer therapy due to their role in cell cycle progression [29]. Also andrographolide structure contains a butyrolactone fragment which is a known CDK inhibitor [30].

In silico studies of the molecules showed many correlations

between the simulated parameters and the observed *in vitro* anti-cancer activity. Moreover, the molecular docking methodology was used to identify the probable structural features like the effect of various substitutents and their positions responsible for the anti-cancer activity in C-12 substituted-14-deoxy-andrographolide derivatives.

MATERIALS AND METHODS

The structures of the proteins were obtained from the Protein Data Bank (PDB) (www.rcsb.org). The PDB IDs are: 1M17 (EGFR tyrosine kinase), 2ITW (EGFR kinase from lung cancer), 1UNL (CDK 5). The C-12 substituted-14-deoxy andrographolide derivatives used for the studies (Figure 1), were modelled using GaussView (3.09) [31].

The energy optimization of these derivatives was carried out using the DFT (631G-B3LYP) theory in Gaussian 03 [32]. The proteins were prepared in MOE [33], by removing the solvent, heteroatoms and the pre-existing ligand molecules. The optimized structures of the andrographolide derivatives were consequently docked with the prepared proteins using Autodock-Vina [34]. The binding interactions in the active sites were then viewed using PyMol [35], and MOE [33]. Finally, these derivatives were evaluated for their drug likeness by determining their Lipinski's parameters at http://www.scfbioiitd.res.in/software/drugdesign/lipinski.jsp [36,37].

RESULTS AND DISCUSSION

Docking studies

The binding energies obtained from the docking studies have been summarized in Table 1 along with the mean *in vitro* growth inhibition in % obtained from the anti-cancer study across the 60 cell line panel of NCI [25].

From the docking studies, the molecule IIIr returned the highest binding energy values in all cases which concurs with its efficacy *in vitro,* with the maximum of growth inhibition (%) demonstrating its potential as a lead [25]. Also the molecule IIIq showed significant binding energies correlating with its observed *in vitro* activity. Similarly, molecule IIIf has the lowest binding affinities and also has nil growth inhibition (%). This lack of activity in IIIf might be due to the long chain octadecyl group. The presence of the long chain alkyl group makes the molecule highly lipophilic. Additionally, the increased steric hindrance results in reduced interaction. Both andrographolide (I) and the triacetyl andrographolide (II) showed significant binding energies but with poor *in vitro* efficacy. In fact andrographolide (I) has a very low growth inhibition (%). The probable cause for this has been attributed to the computed Lipinski's parameters which have been discussed later. Moving forward, we have compared the *in vitro* and *in silico* results with regression analysis without the andrographolide (I) and the triacetyl andrographolide (II) molecules in order to obtain a clear *in vitro* as against the *in silico* correlation. The R^2 values obtained are 1M17 – 0.6839, 1UNl – 0.5688 and 2ITW – 0.7291. The aforementioned significant correlations confirm our level of computational theory. Molecules IIIg, IIIh and IIIi are cycloalkylamines with a cyclopropyl, cyclopentyl and cyclohexyl moieties whereas molecule IIIj has an unsubstituted benzyl amine at C-12. It can be observed from the binding energies and the *in vitro* efficacy that the increase in

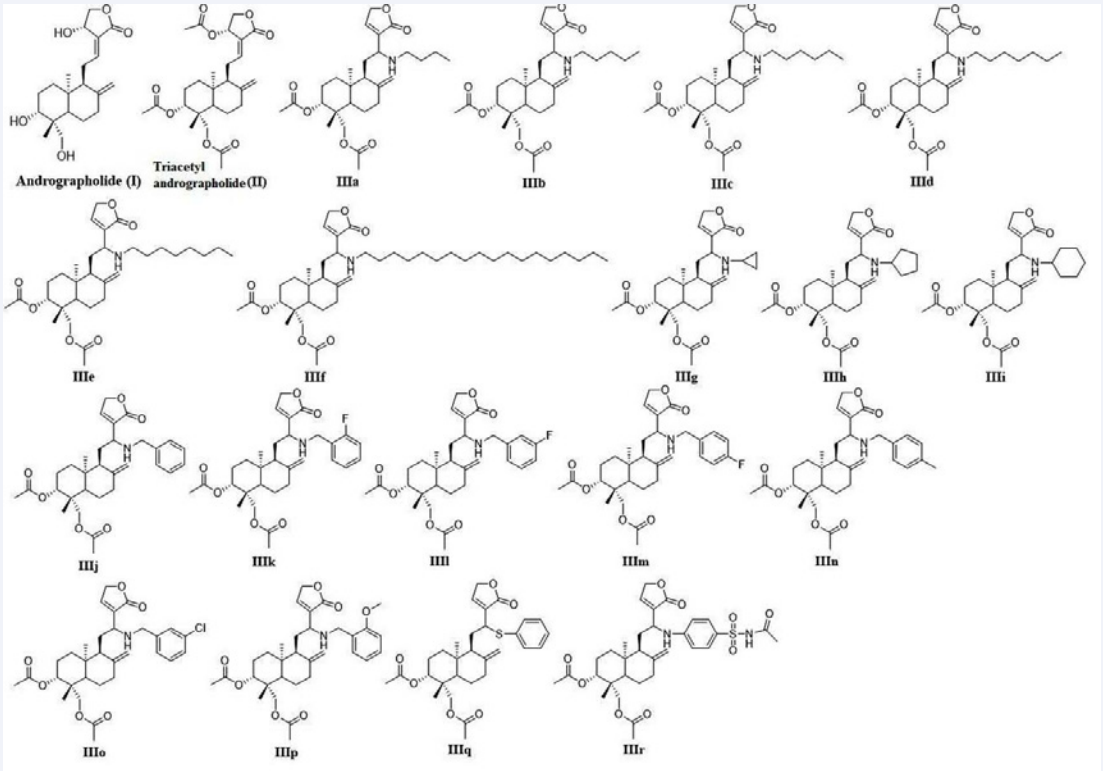

Figure 1 Structures and the codes assigned for the andrographolide derivatives.

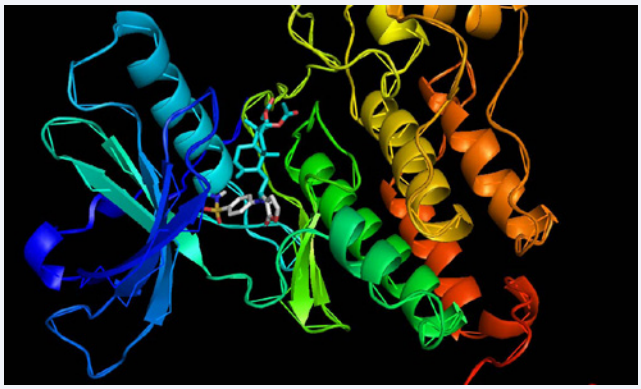

Figure 2 Docked pose of IIIr in 1M17.

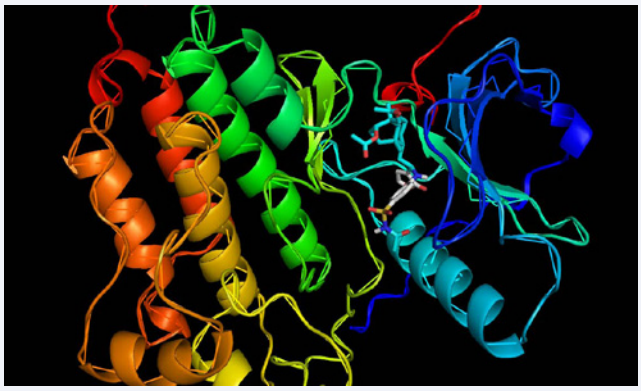

Figure 3 Docked pose of IIIr in 2ITW.

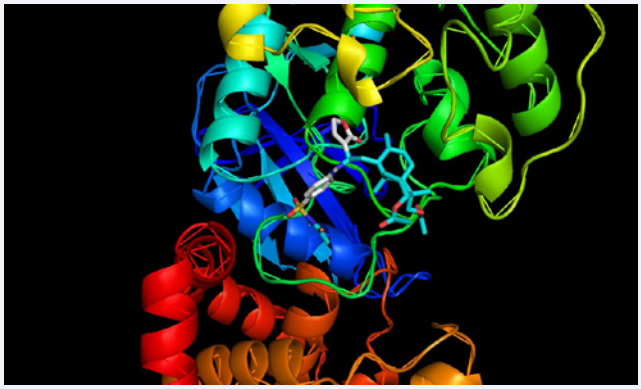

Figure 4 Docked pose of IIIr in 1UNL.

ring size (IIIg to IIIi) and aromaticity (IIIi to IIIj) leads to better activity. IIIk, IIIl, IIIm have fluorine substitution at *ortho*, *meta* and *para* positions respectively. From the docking results it appears that IIIl has higher binding affinities followed by IIIm and then IIIk. This highlights the importance of the position of the substituent, making it as an important finding in our study. Figures 2, 3 and 4 show the best docked poses of IIIr with 1M17, 1UNL and 2ITW respectively.

The *in vitro* SAR (structure activity relationship) findings demonstrated potent activity for the compounds containing the following functionalities at C-12: substituted aryl amino/phenyl thio > benzylamino > alkyl amino. Insertion of sulfonamide substituent to the aryl moiety significantly improved the anti-cancer activity of one of the derivatives (Filed complete specification IN-6104/CHE/2014, 3rd December 2015) (25). Accordingly, in the docking studies, we noted that the average binding affinity values follow the similar trend for 1M17: Aryl amino/phenyl thio (-8.3 kcal/mol) > benzyl amino (-8.1 kcal/mol) > alkyl amino (-7.2 kcal/mol). Therefore as a representative example, we pursued the protein-ligand interactions in the active site for the derivatives against 1M17. Each ligand and its corresponding interacting amino acids have been summarized below in Table 2.

It is quite interesting to note that all the molecules in the study interact with Val 702, Lys 721, Leu 820 and Asp 831. This indicates that andrographolide and its derivatives prefer these amino acids for interaction as a class. These set of amino acid residues appear to be markers in the active site for the andrographolide derivatives. Also in most of the cases Leu 694, Phe 699 and Thr 766 are present. Met 769, Gly 772 and Cys 773 residues are also observed in quite a few cases. Interestingly Asp 776 appears in majority of the molecules containing cyclic moieties. Figure 5 depicts the amino acid interactions with IIIr as observed in MOE.

In case of IIIk, IIIl and IIIm, the position of fluoro substituent varies as *ortho*, *meta* and *para*. This change in the position is reflected with the amino acid interactions also. IIIk having the substitution at *ortho* position interacts with 14 residues as compared to 13 in case of both *meta* (IIIl) and *para* (IIIm). Also both IIIk and IIIm lack the Ala 719 interaction and similarly IIIl and IIIm lack Glu 738 interaction. This indicates that the

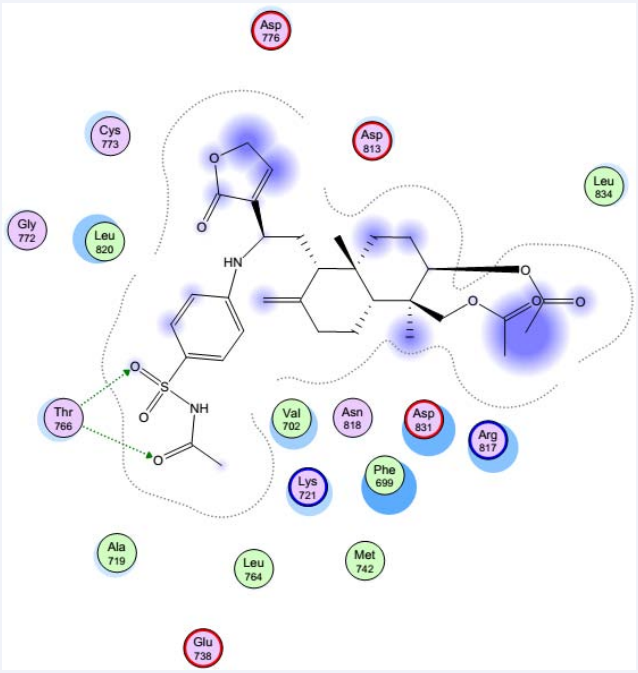

Figure 5 Interacting amino acid residues with IIIr in the active site of 1M17.

Table 1: Binding affinities and *in vitro* activity obtained for the andrographolide derivatives.

Ligand	Binding energy in kcal/mol			Mean % growth inhibition (*in vitro*)
	1M17	1UNl	2ITW	
Andrographolide(I)	-8.0	-6.5	-7.8	17.11
Triacetyl andrographolide(II)	-7.6	-6.3	-7.8	58.91
IIIa	-7.1	-5.6	-7.0	15.68
IIIb	-7.2	-6.4	-6.8	-
IIIc	-7.3	-6.4	-7.2	-
IIId	-7.2	-6.3	-6.6	-
IIIe	-6.7	-6.4	-6.7	33.18
IIIf	-6.1	-6.3	-6.1	0.00
IIIg	-7.5	-6.1	-6.8	4.45
IIIh	-7.6	-6.7	-7.6	31.85
IIIi	-8.1	-6.8	-7.8	-
IIIj	-8.6	-6.9	-8.0	52.83
IIIk	-8.3	-7.0	-7.8	-
IIIl	-8.5	-7.1	-8.0	-
IIIm	-8.4	-6.7	-7.8	55.55
IIIn	-8.1	-6.9	-8.3	-
IIIo	-7.8	-7.1	-7.6	47.89
IIIp	-7.1	-6.9	-8.3	-
IIIq	-8.3	-6.6	-7.7	89.86
IIIr	-9.0	-7.7	-8.5	100.00

Note: '-'indicates that the molecules were not tested *in vitro*

Table 2: Ligands with their respective interacting amino acid residues in the active site of 1M17.

Ligand	Interacting amino acids in the active site
Andrographolide(I)	Val 702, Ala 719, Ile 720, Lys 721, Glu 738, Met 742, Leu 764, Thr 766, Cys 773, Arg 17, Leu 820, Asp 831
Triacetyl andrographolide (II)	Leu 694, Phe 699, Val 702, Ala 719, Lys 721, Thr 766, Gln 767, Leu 768, Met 769, Gly 772, Cys 773, Arg 817, Leu 820, Asp 831
IIIa	Leu 694, Phe 699, Val 702, Ala 719, Lys 721, Thr 766, Met 769, Pro 770, Gly 772, Cys 773, Arg 817, Leu 820, Asp 831
IIIb	Gly 695, Gly 697, Phe 699, Val 702, Ala 719, Lys 721, Met 742, Thr 766, Gln 767, Leu 768, Met 769, Cys 773, Arg 817, Leu 820, Thr 830, Asp 831
IIIc	Leu 694, Gly 695, Phe 699, Val 702, Lys 721, Thr 766, Met 769, Gly 772, Cys 773, Asp 776, Leu 820, Asp 831
IIId	Leu 694, Phe 699, Val 702, Ala 719, Lys 721, Thr 766, Met 769, Gly 772, Cys 773, Arg 817, Leu 820, Thr 830, Asp 831
IIIe	Leu 694, Gly 695, Phe 699, Val 702, Ala 719, Lys 721, Glu 738, Met 742, Leu 764, Thr 766, Met 769, Gly 772, Cys 773, Arg 817, Leu 820, Thr 830, Asp 831
IIIf	Leu 694, Gly 695, Phe 699, Val 702, Ala 719, Lys 721, Thr 766, Met 769, Gly 772, Arg 817, Asn 818, Leu 820, Asp 831
IIIg	Leu 694, Gly 695, Ser 696, Gly 697, Phe 699, Val 702, Ala 719, Lys 721, Thr 766, Met 769, Cys 773, Asp 776, Arg 817, Leu 820, Thr 830, Asp 831
IIIh	Leu 694, Gly 695, Phe 699, Val 702, Lys 721, Met 769, Gly 772, Cys 773, Asp 776, Leu 820, Asp 831
IIIi	Leu 694, Gly 695, Ser 696, Gly 697, Phe 699, Val 702, Ala 719, Lys 721, Glu 738, Thr 766, Gln 767, Leu 768, Met 769, Gly772, Cys 773, Leu 820, Thr 830, Asp 831
IIIj	Leu 694, Gly 695, Phe 699, Val 702, Ala 719, Lys 721, Thr 766, Met 769, Gly772, Cys 773, Asp 776, Leu 820, Thr 830, Asp 831
IIIk	Leu 694, Gly 695, Phe 699, Val 702, Lys 721, Glu 738, Thr 766, Met 769, Gly772, Cys 773, Asp 776, Leu 820, Thr 830, Asp 831
IIIl	Leu 694, Gly 695, Phe 699, Val 702, Ala 719, Lys 721, Thr 766, Met 769, Gly772, Cys 773, Asp 776, Leu 820, Asp 831
IIIm	Leu 694, Gly 695, Phe 699, Val 702, Lys 721, Thr 766, Met 769, Gly772, Cys 773, Asp 776, Leu 820, Thr 830, Asp 831
IIIn	Leu 694, Gly 695, Ser 696, Gly 697, Phe 699, Val 702, Ala719, Lys 721, Thr 766, Leu 768, Met 769, Pro 770, Gly772, Asp 776, Leu 820, Asp 831
IIIo	Leu 694, Gly 695, Ser 696, Gly 697, Phe 699, Val 702, Lys 721, Thr 766, Gly772, Cys 773, Leu 820, Asp 831
IIIp	Leu 694, Phe 699, Val 702, Lys 721, Thr 766, Asp 813, Arg 817, Asn 818, Leu 820, Asp 831
IIIq	Leu 694, Gly 695, Ser 696, Gly 697, Phe 699, Val 702, Ala 719, Lys 721, Glu 738, Met 742, Leu 764, Thr 766, Gln 767, Met 769, Leu 820, Asp 831
IIIr	Phe 699, Val 702, Ala 719, Lys 721, Glu 738, Met 742, Leu 764, Thr 766, Gly 772, Cys 773, Asp 776, Asp 813, Arg 817, Asn 818, Leu 820, Asp 831, Leu 834

Table 3: Computed Lipinski's parameters for the andrographolide derivatives.

Ligand	Molecular mass (Daltons)	No. of hydrogen bond donor(s)	No. of hydrogen bond acceptor(s)	Log P	Molar refractivity
Andrographolide(I)	312	5	6	-0.053	77.15
Triacetyl andrographolide(II)	458	0	8	2.642	104.49
IIIa	467	0	6	2.826	115.39
IIIb	479	0	6	2.171	119.52
IIIc	491	0	6	2.646	120.25
IIId	505	0	6	2.987	125.64
IIIe	517	0	6	3.381	130.05
IIIf	647	0	6	5.640	174.72
IIIg	453	0	6	2.128	108.05
IIIh	477	0	6	1.983	113.74
IIIi	489	0	6	2.415	115.82
IIIj	501	0	6	2.744	121.46
IIIk	519	0	6	3.161	121.66
IIIl	521	0	6	3.250	123.78
IIIm	521	0	6	3.212	124.45
IIIn	517	0	6	3.303	129.43
IIIo	517	0	6	3.341	128.77
IIIp	531	0	7	2.808	127.48
IIIq	506	0	6	2.770	120.00
IIIr	610	0	9	2.203	139.72

position of the substituent indeed affects the interactions. The effect of type of substituent also is seen when we compare IIIl (*meta* fluoro) and IIIo (*meta* chloro) where a few interactions differ. Similarly IIIk (*ortho* fluoro) and IIIp (*ortho* methoxy), IIIm (*para* fluoro) and IIIn (*para* methyl) also have shown different interactions with different substitutions at the same position.

Lipinski's parameters

The synthesized andrographolide derivatives were also evaluated for Lipinski's parameters (logP (partition coefficient), molecular mass (daltons), number of hydrogen donor(s), number of hydrogen acceptor(s) and molar refractivity) using the online tool available in http://www.scfbioiitd.res.in/software/drugdesign/lipinski.jsp. The likeness score of the andrographolide derivatives are tabulated in Table 3.

Many of the andrographolide derivatives complied with the Lipinski's parameters further emphasizing the fact that these C-12 substituted andrographolide derivatives can be explored as potential anti-cancer drugs. This is reflected in the computed logP values and the number of hydrogen bond donor(s)/acceptor(s). LogP (partition coefficient) values of many of these derivatives fall in the range of 2 - 3 signifying a good balance between their lipophilicity and hydrophilicity. The number of hydrogen bond donors (below 5) and acceptors (below 10)fall within the expected range [36,37], indicating a significant number of interactions between the drug and the active site in the protein.

Significant difference in the molar refractivity and the logP values were observed between andrographolide (I) and the triacetyl andrographolide (II). Further, there are 8 hydrogen bond acceptors in the triacetyl andrographolide molecule as compared to 6 in the andrographolide molecule. These two factors probably explain the better *in vitro* efficacy of triacetyl andrographolide (II) as against andrographolide (I).

CONCLUSION

In this *in silico* study, we modeled C-12 substituted-14-deoxy-andrographolide derivatives which have been evaluated for their *in vitro* anti-cancer activity. We observed the conformity of the *in silico* results in resonance with the *in vitro* results. This study provided the probable targets for the site of anti-cancer action of these derivatives. We have further established the interacting amino acids residues in the active site of the EGFR tyrosine kinase protein (1M17). The docking studies and the interacting amino acids thus helped visualize the effect of substituents and their position on the anti-cancer efficacy. Finally, the compliance to Lipinski's parameters demonstrated that many of these C-12 substituted-14-deoxy andrographolide derivatives can be explored as potential leads in further drug discovery.

ACKNOWLEDGEMENTS

The authors are grateful to Bhagawan Sri Sathya Sai Baba, Founder Chancellor, SSSIHL, for His constant inspiration. We also thank SSSIHL molecular modelling lab for providing the facilities. The authors also thank Sri Parth Gupta (IIT-Chennai) for his help with the MOE software.

REFERENCES

1. Hazra A, Paira P, Sahu KB, Naskar S, Saha P, Paira R, et al. Chemistry of andrographolide: formation of novel di-spiropyrrolidino and di-spiropyrrolizidino-oxindole adducts via one-pot three-component

[3+2] azomethine ylide cycloaddition. Tetrahedron Lett. 2010; 51: 1585-1588.

2. Brahmachari G. Andrographolide: A Molecule of Antidiabetic Promise. Discov Dev Antidiabetic Agents from Nat Prod Nat Prod Drug Discov. 2016; 1.

3. Puri A, Saxena R, Saxena RP, Saxena KC, Srivastava V, Tandon JS. Immunostimulant agents from Andrographis paniculata. J Nat Prod. 1993; 56: 995-999.

4. Wang T, Liu B, Zhang W, Wilson B, Hong J-S. Andrographolide reduces inflammation-mediated dopaminergic neurodegeneration in mesencephalic neuron-glia cultures by inhibiting microglial activation. J Pharmacol Exp Ther. 2004; 308: 975-983.

5. Pandeti S, Sonkar R, Shukla A, Bhatia G, Tadigoppula N. Synthesis of new andrographolide derivatives and evaluation of their antidyslipidemic, LDL-oxidation and antioxidant activity. Eur J Med Chem. 2013; 69: 439-448.

6. Lee JC, Tseng CK, Young KC, Sun HY, Wang SW, Chen WC, et al. Andrographolide exerts anti-hepatitis C virus activity by up-regulating haeme oxygenase-1 via the p38 MAPK/Nrf2 pathway in human hepatoma cells. Br J Pharmacol. 2014; 171: 237-252.

7. Nanduri S, Nyavanandi VK, Thunuguntla SSR, Velisoju M, Kasu S, Rajagopal S, et al. Novel routes for the generation of structurally diverse labdane diterpenes from andrographolide. Tetrahedron Lett. 2004; 45: 4883-4886.

8. Nanduri S, Nyavanandi VK, Thunuguntla SSR, Kasu S, Pallerla MK, Ram PS, et al. Synthesis and structure--activity relationships of andrographolide analogues as novel cytotoxic agents. Bioorg Med Chem Lett. 2004; 14: 4711-4717.

9. Kumar RA, Sridevi K, Kumar NV, Nanduri S, Rajagopal S. Anticancer and immunostimulatory compounds from Andrographis paniculata. J Ethnopharmacol. 2004; 92: 291-295.

10. Preet R, Chakraborty B, Siddharth S, Mohapatra P, Das D, Satapathy SR, et al. Synthesis and biological evaluation of andrographolide analogues as anti-cancer agents. Eur J Med Chem. 2014; 85: 95-106.

11. Jada SR, Hamzah AS, Lajis NH, Saad MS, Stevens MFG, Stanslas J. Semisynthesis and cytotoxic activities of andrographolide analogues. J Enzyme Inhib Med Chem. 2006; 21: 145-155.

12. Devendar P, Nayak VL, Yadav DK, Kumar AN, Kumar JK, Srinivas KVNS, et al. Synthesis and evaluation of anticancer activity of novel andrographolide derivatives. Med chem comm. 2015; 6: 898-904.

13. Chakraborty D, Maity A, Jain CK, Hazra A, Bharitkar YP, Jha T, et al. Cytotoxic potential of dispirooxindolo/acenaphthoquino andrographolide derivatives against MCF-7 cell line. Med chem comm. 2015; 6: 702-707.

14. Peng Y, Li J, Sun Y, Chan JY-W, Sheng D, Wang K, et al. SAR studies of 3, 14, 19-derivatives of andrographolide on anti-proliferative activity to cancer cells and toxicity to zebra fish: an in vitro and in vivo study. RSC Adv. 2015; 5: 22510-22526.

15. Jada SR, Subur GS, Matthews C, Hamzah AS, Lajis NH, Saad MS, et al. Semisynthesis and in vitro anticancer activities of andrographolide analogues. Phytochemistry. 2007; 68: 904-912.

16. Kasemsuk S, Sirion U, Suksen K, Piyachaturawat P, Suksamrarn A, Saeeng R. 12-Amino-andrographolide analogues: synthesis and cytotoxic activity. Arch Pharm Res. 2013; 36: 1454-1464.

17. Sirion U, Kasemsook S, Suksen K, Piyachaturawat P, Suksamrarn A, Saeeng R. New substituted C-19-andrographolide analogues with potent cytotoxic activities. Bioorg Med Chem Lett. 2012; 22: 49-52.

18. Das B, Chowdhury C, Kumar D, Sen R, Roy R, Das P, et al. Synthesis, cytotoxicity, and structure--activity relationship (SAR) studies of andrographolide analogues as anti-cancer agent. Bioorg Med Chem Lett. 2010; 20: 6947-6950.

19. Rajagopal S, Kumar RA, Deevi DS, Satyanarayana C, Rajagopalan R. Andrographolide, a potential cancer therapeutic agent isolated from Andrographis paniculata. J Exp Ther Oncol. 2003; 3: 147-158.

20. Sirion U, Kasemsuk T, Piyachaturawat P, Suksen K, Suksamrarn A, Saeeng R. Synthesis and cytotoxic activity of 14-deoxy-12-hydroxyandrographolide analogs. Med Chem Res. 2017; 1-11.

21. Chen D, Song Y, Lu Y, Xue X. Synthesis and in vitro cytotoxicity of andrographolide-19-oic acid analogues as anti-cancer agents. Bioorg Med Chem Lett. 2013; 23: 3166-3169.

22. Jada SR, Matthews C, Saad MS, Hamzah AS, Lajis NH, Stevens MFG, et al. Benzylidene derivatives of andrographolide inhibit growth of breast and colon cancer cells in vitro by inducing G1 arrest and apoptosis. Br J Pharmacol. 2008; 155: 641-654.

23. Wei S, Tang YB, Hua H, Ohkoshi E, Goto M, Wang LT, et al. Discovery of novel andrographolide derivatives as cytotoxic agents. Bioorg Med Chem Lett. 2013; 23: 4056-4060.

24. Wu ZW, Xu HW, Dai GF, Liu MJ, Zhu LP, Wu J, et al. Improved inhibitory activities against tumor-cell migration and invasion by 15-benzylidene substitution derivatives of andrographolide. Bioorg Med Chem Lett. 2013; 23: 6421-6426.

25. Kandanur SGS, Golakoti NR, Nanduri S. Synthesis and in vitro cytotoxicity of novel C-12 substituted-14-deoxy-andrographolide derivatives as potent anti-cancer agents. Bioorganic Med Chem Lett. 2015; 25: 5781-5786.

26. Levita J, Nawawi A ari, Mutalib A, Ibrahim S. Andrographolide: a review of its anti-inflammatory activity via inhibition of NF-kappaB activation from computational chemistry aspects. Int J Pharmacol. 2010; 6: 569-576.

27. Uttekar MM, Das T, Pawar RS, Bhandari B, Menon V, Gupta SK, et al. Anti-HIV activity of semisynthetic derivatives of andrographolide and computational study of HIV-1 gp120 protein binding. Eur J Med Chem. 2012; 56: 368-374.

28. Al-Suwaidan IA, Abdel-Aziz NI, El-Azab AS, El-Sayed MA-A, Alanazi AM, El-Ashmawy MB, et al. Antitumor evaluation and molecular docking study of substituted 2-benzylidenebutane-1, 3-dione, 2-hydrazonobutane-1, 3-dione and trifluoromethyl-1H-pyrazole analogues. J Enzyme Inhib Med Chem. 2015; 30: 679-687.

29. Mapelli M, Massimiliano L, Crovace C, Seeliger MA, Tsai LH, Meijer L, et al. Mechanism of CDK5/p25 binding by CDK inhibitors. J Med Chem. 2005; 48: 671-679.

30. Kitagawa M, Higashi H, Takahashi IS, Okabe T, Ogino H, Taya Y, et al. A cyclin-dependent kinase inhibitor, butyrolactone I, inhibits phosphorylation of RB protein and cell cycle progression. Oncogene. 1994; 9: 2549-2557.

31. Dennington R, Keith T, Millam J, Eppinnett K, Hovell WL, Gilliland RG, et al. Version 3.09. Semichem. Inc, Shawnee Mission KS. 2003.

32. Frisch MJ, Trucks GW, Schlegel HB, Scuseria GE, Robb MA, Cheeseman JR, et al. Gaussian 03, revision C. 02; Gaussian, Inc.: Wallingford, CT, 2004. There is no Corresp Rec this Ref. 2013.

33. Molecular Operating Environment (MOE). 1010 Sherbooke St. West, Suite #910, Montreal, QC, Canada, H3A 2R7: Chemical Computing Group Inc. 2017.

34. Trott O, Olson AJ. AutoDock Vina: improving the speed and accuracy of docking with a new scoring function, efficient optimization, and multithreading. J Comput Chem. 2010; 31: 455-461.

35. DeLano WL. The PyMOL Molecular Graphics System, Version 1.7. 4. Schr{ö}dinger, LLC. 2015.

36. Lipinski CA. Lead-and drug-like compounds: the rule-of-five revolution. Drug Discov Today Technol. 2004; 1: 337-341.

37. Jayaram B, Singh T, Mukherjee G, Mathur A, Shekhar S, Shekhar V. Sanjeevini: a freely accessible web-server for target directed lead molecule discovery. BMC Bioinformatics. 2012; 13: S7.

Cite this article

Kar S, Manohar CS, Sarma Kandanur SG, Nanduri S, Belliraj SK, et al. (2017) In silico Modeling of New C-12 Substituted-14-Deoxy-Andrographolide Derivatives as Potent Anticancer Leads. J Pharmacol Clin Toxicol 5(4):1083.